Acetogenin Cytotoxicity

DOI: 10.1002/anie.201100717

The Calcium-Chelating Capability of Tetrahydrofuranic Moieties Modulates the Cytotoxicity of Annonaceous Acetogenins**

Chih-Chuang Liaw, Wen-Ying Liao, Chien-Sheng Chen, Shu-Chuan Jao, Yang-Chang Wu, Chia-Ning Shen,* and Shih-Hsiung Wu**

Annonaceous acetogenins (AGEs) are potential phytochemicals of herbal medicines and exhibit a wide variety of biological activities.[1] Recent work has demonstrated that AGEs have a cytotoxic potency comparable to that of Taxol.[2] AGEs belong to a unique class of polyketides with a C_{35} or C_{37} aliphatic chain terminated by an α,β-unsaturated γ-lactone group on one end and interrupted mid-chain by one or two tetrahydrofuran (THF) rings with hydroxy groups (Scheme 1).[3] Both structural groups have been recognized as the pharmacophores that block electron transport in mitochondrial complex I.[4]

Efforts to clarify the targeting and mechanism of AGEs include altering the space between two moieties,[5] removing either one of two critical moieties (ΔLac acetogenins or muricatacin), mimicking the THF moieties by ether linkage,[6] connecting a fluorescent group at the end of the aliphatic chain[7] or with a hydroxy group, or replacing the γ-lactone moiety by a fluorescent group.[4a,8] Hemisynthetic and proteomic techniques to clarify the mechanism underlying the action of AGEs have suggested some cytosolic and reticulum-associated enzymes as putative targets of AGEs.[9] Besides, as the natural ionophore calcimycin A23187,[10] the hydroxylated bis-THF moieties of AGEs were shown to form complexes with bivalent cations, such as Ca^{2+} and Mg^{2+}.[11] Although some of these modified AGEs obtained thus far have demonstrated activities comparable to those of naturally occurring AGEs, the critical mechanism underlying the cytotoxic actions of AGEs has not yet been fully clarified.

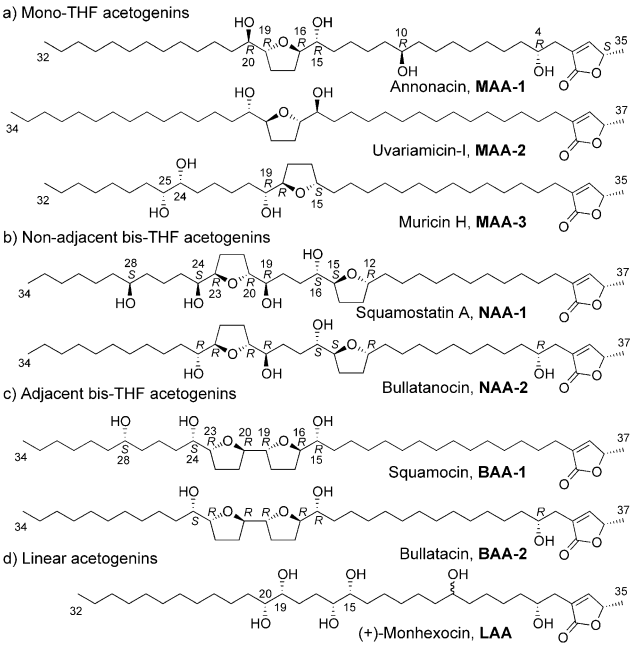

Scheme 1. Chemical structures of selected AGEs, isolated from Formosan annonaceous plants.

Earlier ^{1}H NMR studies have revealed that synthesized hydroxylated adjacent bis-THF derivatives (partial cores of AGEs) and the adjacent bis-THF AGEs, bullatacin (**BAA-2**) and asimicin, are able to chelate Ca^{2+} ions from $Ca(SCN)_2$ in a 2:1 ratio.[11a,b] Other studies based on ^{13}C NMR longitudinal relaxation time (T_1) have also shown that annonacin (**MAA-1**) and squamocin (**BAA-1**) undergo structural changes while chelating Ca^{2+} ions (Figure 1).[12] To determine how Ca^{2+} forms complexes with AGEs, we used calcium perchlorate and found that the proton signals of the THF cores in the calcium complexes of **MAA-1** and **BAA-1** shifted downfield relative to calcium-free molecules (Figure 1a–c and Figures S1–S3 in the Supporting Information).

We determined the stoichiometry of the AGE/Ca^{2+} complex by calorimetry (see below). From ^{1}H NMR studies,

[*] Dr. C.-C. Liaw
Department of Marine Biotechnology and Resources
National Sun Yat-sen University
70 Lienhai Road, Kaohsiung 80424 (Taiwan)
E-mail: ccliaw@mail.nsysu.edu.tw
Dr. C.-C. Liaw, W.-Y. Liao[+]
Graduate Institute of Pharmaceutical Chemistry
China Medical University
91 Hsueh-Shih Road, Taichung 40402 (Taiwan)
W.-Y. Liao,[+] Dr. C.-N. Shen
Genomics Research Centre, Academia Sinica
128 Academia Road, Sec. 2, Taipei 115 (Taiwan)
E-mail: cnshen@gate.sinica.edu.tw
Dr. C.-S. Chen, Dr. S.-C. Jao, Prof. S.-H. Wu
Institute of Biological Chemistry, Academia Sinica
128 Academia Road, Sec. 2, Taipei 115 (Taiwan)
E-mail: shwu@gate.sinica.edu.tw
Prof. Y.-C. Wu[+]
Graduate Institute of Integrate Medicine, China Medical University
91 Hsueh-Shih Road, Taichung 40402 (Taiwan)
[+] These authors contributed equally.

[**] We thank Li-Wen Lo for assistance with confocal microscopy (Genomics Research Centre, Academia Sinica) and Dr. YuLin Lam (National University of Singapore) for English editing. This work was supported in part by National Science Council grant NSC97-2320-B-039-018-MY3 and Ministry of Education grant 97C031702 to C.-C.L. and by Academia Summit Project grant no. 5202402020-0 to C.-N.S. and no. 5202401023-2 to S.-H.W.
Supporting information for this article is available on the WWW under http://dx.doi.org/10.1002/anie.201100717.

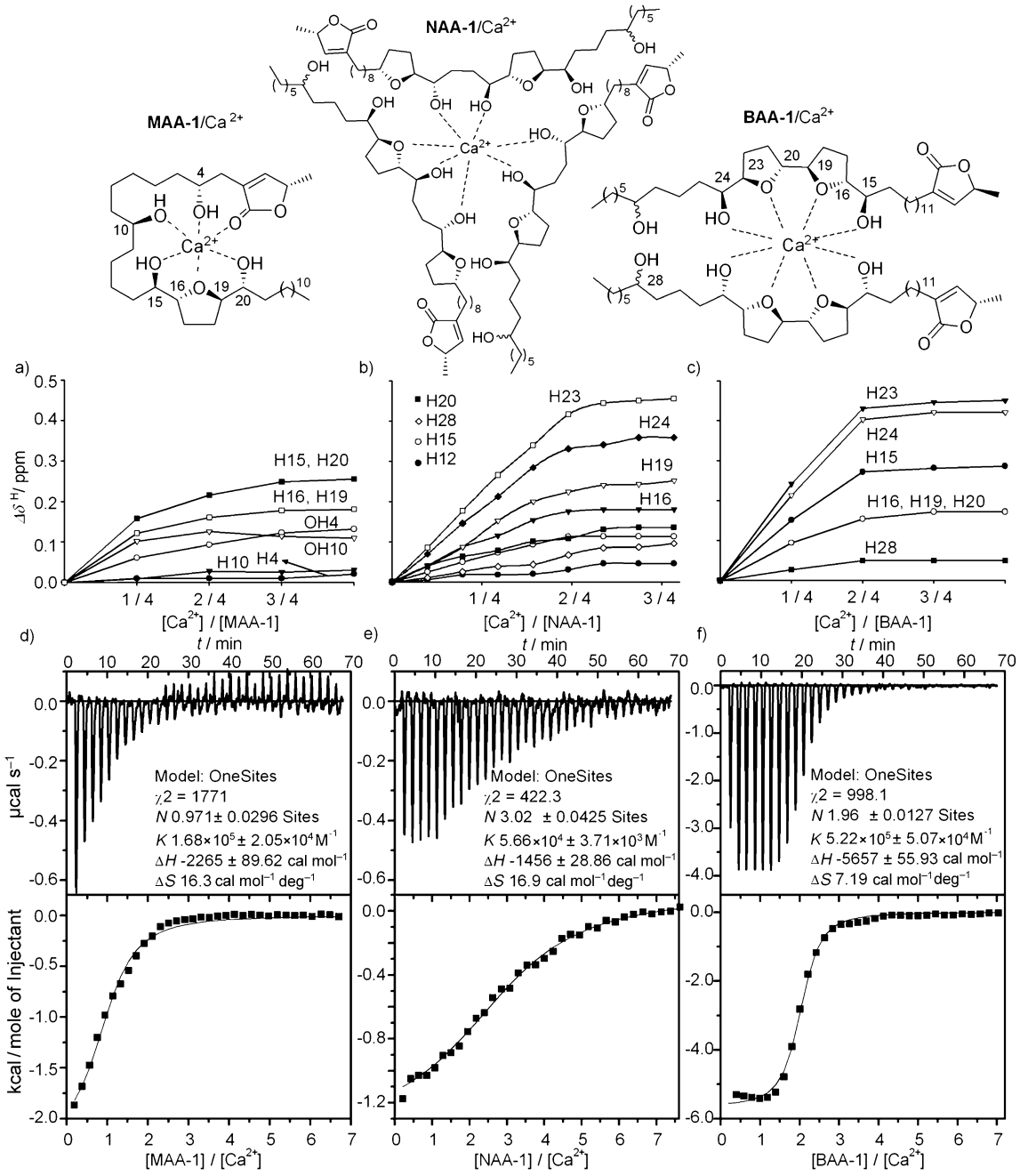

Figure 1. Representative structures, changes in the NMR signals, and ITC titrations of the AGE/Ca^{2+} complexes. The AGEs (1.5 mM) **MAA-1** (a), **NAA-1** (b), and **BAA-1** (c) were titrated with calcium ions at the molar ratios indicated. $\Delta\delta_H = \delta_H[Ca^{2+}/AGE] - \delta_H[AGE]$, in ppm. ITC titrations of d) 30 μM Ca^{2+} with 1 mM **MAA-1** in $CH_3CN/CHCl_3$ (1:1, v/v), e) 30 μM Ca^{2+} with 1 mM **NAA-1** in CH_3CN, and f) 65 μM Ca^{2+} with 1 mM **BAA-1** in CH_3CN were performed using an ITC microcalorimeter at 25 °C. χ^2, nonlinear least-squares algorithm; *N*, number of binding sites; *K*, association constant; ΔH, enthalpy change; ΔS, entropy change. For each titration, raw data were obtained from 33 automatic injections (8 μL per injection), and the integrated fitted curves show the experimental points with a one-site fitting function.

the signals of H-15/20 and H-16/19 (with *threo* configuration) of the α-hydroxylated THF core of **MAA-1** were shifted downfield by 0.26 and 0.18 ppm, and those of OH-4 and OH-10 were shifted downfield by 0.13 and 0.11 ppm, respectively. With one additional carbonyl group of the γ-lactone moiety,[12] six polar ligands of **MAA-1** could provide the calcium-chelating ability.

From ^{1}H NMR spectroscopy, the signals for H-23/24 (with *erythro* configuration) of **BAA-1** were shifted downfield by 0.45 and 0.42 ppm, respectively, while the downfield changes of 2.7 and 1.9 ppm in the signals of H-15/16 (with *threo* configuration) showed a pattern similar to that of **MAA-1**. These proton signal shifts are attributed to the conformational change of the THF moiety caused by the neighboring hydroxy group involved in formation of the chelating com-

plex. Without the additional hydroxy groups, eight polar functional groups from two **BAA-1** molecules were assumed to be involved in chelating calcium.

We also observed conformational changes in the nonadjacent bis-THF AGE squamostatin A (**NAA-1**), when the Ca^{2+} concentration was increased by the ^1H NMR study. The signals for the *erythro* H-23/24 of **NAA-1** shifted downfield by 0.45 and 0.36 ppm, respectively; the H-19 and H-16 signals of H-19/20 and H-16/15 with *threo* configuration were shifted downfield by 0.25 and 0.16 ppm, respectively. These shifts indicated that the THF moiety flanking the hydroxy groups of **NAA-1**, along with the THF moiety with a *threo* hydroxy group, was critical for the formation of calcium-chelating complexes. The changes in the NMR signals demonstrated that the THF cores of AGEs interact with Ca^{2+}, thereby altering the complex conformation of the AGEs. On the other hand, H-28 of **BAA-1** and **NAA-1** was slightly shifted by 0.05 and 0.1 ppm, respectively, which might be induced by an anisotropic effect of the AGE/Ca^{2+} complexes.

Isothermal titration calorimetry (ITC) measures thermal responses and the binding kinetics of biomolecules and metal ions in solution.[13] We used ITC to elucidate the interaction between AGEs and Ca^{2+} ions.[14] Four types of bioactive AGEs were selected (see Scheme 1): 1) the mono-THF AGEs annonacin (**MAA-1**), uvariamicin-I (**MAA-2**), and muricin H (**MAA-3**); 2) the nonadjacent bis-THF AGEs squamostatin A (**NAA-1**) and bullatanocin (**NAA-2**); 3) the adjacent bis-THF AGEs squamocin (**BAA-1**) and bullatacin (**BAA-2**); and 4) the linear AGE (+)-monhexocin (**LAA**). The binding properties and stoichiometry of the selected AGEs complexed with Ca^{2+} ions were confirmed by ITC (Figure 1 d–f and Figures S4–S6 in the Supporting Information). The negative enthalpy indicated that the formation of AGE/Ca^{2+} complexes was an exothermic process with increasing entropy, thus contributing to the spontaneous interaction.

Based on titrations of soluble calcium ions with selected AGEs, the ITC curves were categorized into three patterns of Ca^{2+} chelation with AGEs: from the points of reflection of the fitting curves, the molar ratio of **MAA-1**/Ca^{2+} was 1, that of **NAA-1**/Ca^{2+} was 3, and that of **BAA-1**/Ca^{2+} was 2. From the optimal one-site curve fitting to the points of reflection, the association constants obtained for different AGE/Ca^{2+} complexes were at least $10^4\,M^{-1}$ in magnitude, which is larger than that for the **BAA-1**/Ca^{2+} complex ($10^3\,M^{-1}$, obtained from NMR titration data),[12] which implied that the hydrophobic interaction between the aliphatic chains of the AGEs stabilizes the complexes to bundle calcium ions with the core THF moieties. In contrast, the ITC patterns of **LAA** (without a THF moiety) and **MAA-3** (with only one hydroxy group flanking the THF moiety) indicated that neither type of AGE chelates Ca^{2+} ions (Figure S5 in the Supporting Information), which demonstrated that the hydroxy groups flanking both sides of the THF moiety play important roles in the formation of the AGE/Ca^{2+} complex.

The binding molar enthalpy of the **BAA-1**/Ca^{2+} complex was 5.6 kcal mol^{-1} and larger than that of **MAA-1**/Ca^{2+} (2.3 kcal mol^{-1}). The binding molar entropy of **BAA-1**/Ca^{2+} was 7.2 cal mol^{-1} K^{-1}, generated largely from the solvent molecules excluded from the complexes. The entropy of **MAA-1**/Ca^{2+} was 16.3 cal mol^{-1} K^{-1}, and this larger value was a result of both solvent exclusion and the conformational change of **MAA-1**. This larger conformational change after complex formation with calcium at a 1:1 ratio could be explained by the polar functional groups of **MAA-1** chelating with Ca^{2+}, thereby changing the linear **MAA-1** into a curved **MAA-1**/Ca^{2+} complex (Figure 1). Without the polar functional groups OH-4 and OH-10, the binding molar ratio of **MAA-2**/Ca^{2+} was 2 and the binding entropy was 9.7 cal mol^{-1} K^{-1}, which reflected a lesser conformational change. This result could also indicate that **NAA-1**/Ca^{2+} at a 3:1 ratio changes the linear molecules to a highly packaged structure and would explain the higher entropy (16.9 cal mol^{-1} K^{-1}).

Because of the formation of the chelating complex between AGEs and Ca^{2+}, we hypothesized that the Ca^{2+} chelation of THF moieties could mediate the cytotoxicity of AGEs by disrupting intracellular calcium homeostasis. We tested this hypothesis by using three AGEs conspicuously cytotoxic toward HepG2 liver cancer cells, **MAA-1**, **NAA-1**, and **BAA-1**, with IC_{50} values of 7.4, 1.4, and 0.057 nM, respectively (Table S1 in the Supporting Information). We found that the addition of AGEs significantly reduced cell survival because of an increase in the apoptosis rate (Figure 2 and Figure S7 in the Supporting Information). In contrast, the survival rate of HepG2 cells significantly increased by 48, 35, and 43% when 10 nM ethylenediaminetetraacetic acid (EDTA) was added together with 10 nM **MAA-1**, 10 nM **NAA-1**, and 1 nM **BAA-1**, respectively (Figure 2). This could be attributed to EDTA competitively chelating with Ca^{2+} ions and thus decreasing the formation of AGE/Ca^{2+} complexes, which then reduced the disturbance of intracellular levels of calcium and the cytotoxicity of AGEs.

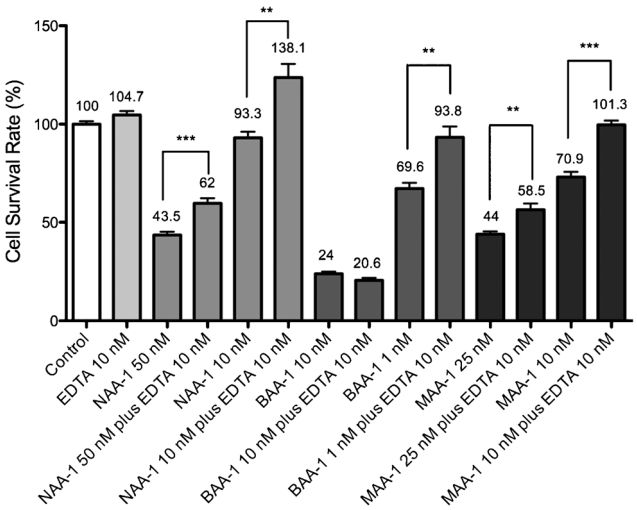

Figure 2. HepG2 cells treated with the indicated concentrations of **NAA-1**, **BAA-1**, and **MAA-1** for 48 h, with or without preincubation with 10 nM EDTA. Cell survival rate was determined based on results of the MTT assay. All experiments were carried out in triplicate. Bars denote standard deviations. The statistical significance was set at $*p < 0.05$, $**p < 0.01$, $***p < 0.001$.

We then examined whether intracellular calcium levels were affected by preincubation of the cells with **BAA-1**, **NAA-1**, or **MAA-1**. Intracellular calcium in AGE-treated HepG2 cells was visualized by the cell-permeable indicator dye, Fluo-4 AM, together with the mitochondrial probe, MitoTracker Red. The culture medium of HepG2 cells contained 1.05 mM $CaCl_2$. A 10 min preincubation of HepG2 cells with 50 μM **BAA-1**, **NAA-1**, or **MAA-1** resulted in a fivefold increase in Fluo-4 AM fluorescence (Figure 3,

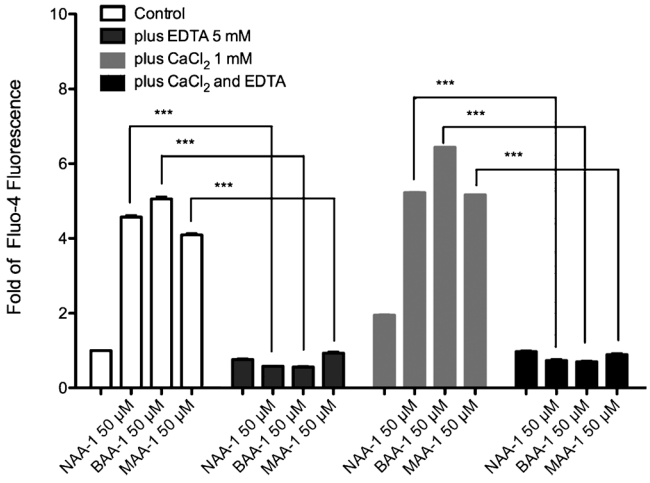

Figure 3. AGEs increase the intracellular level of calcium. HepG2 cells cultured in medium containing 1.05 mM $CaCl_2$ were preincubated with one AGE (**NAA-1**, **BAA-1**, or **MAA-1** at 50 μM) for 10 min with or without exogenous addition of 5 mM EDTA or 1 mM $CaCl_2$. The cells were then stained with Fluo-4 AM. The changes in calcium levels are indicated as fold changes in the optical density value. All experiments were carried out in triplicate. Bars denote standard deviations. The statistical significance was set at $*p<0.05$, $**p<0.01$, $***p<0.001$.

$p<0.001$), which indicated that preincubation of AGEs increased the intracellular levels of calcium in HepG2 cells. Exogenous addition of 1 mM $CaCl_2$ slightly increased the intracellular level of calcium in both untreated and AGE-treated cells. In contrast, the effect of the AGE-mediated increase in intracellular levels of calcium was blocked when HepG2 cells were preincubated with 5 mM EDTA (Figure 3).

Time-lapse confocal microscopy further demonstrated that Fluo-4 AM fluorescence first accumulated in the cytoplasm. After incubation with bis-THF AGEs, the Fluo-4 AM green fluorescence was co-localized with the Mito-Tracker Red fluorescence, which suggests that some cytosolic Ca^{2+} was transported into the mitochondria (Figure 4 a–d and Figure S8 in the Supporting Information). To address whether the Ca^{2+} concentration inside mitochondria was changed by preincubation with AGEs, we used the selective indicator dye for mitochondrial Ca^{2+}, Rhod-2/AM, to evaluate changes in levels of mitochondrial calcium. As shown in Figure 4 e–h, a 10-minute exposure of HepG2 cells to 50 μM **BAA-1** or **NAA-1** caused an increase in the level of mitochondrial calcium. In contrast, incubation of HepG2 with **MAA-1** did not significantly alter the levels of mitochondrial calcium. These results, coupled with the revelation that addition of EDTA counteracted the increase in mitochondrial Ca^{2+} fluorescence induced by preincubation with **BAA-1** or **NAA-1** (Figure 4 i–l and Figure S9 in the Supporting Information), suggested not only that the AGEs bind Ca^{2+} ions but also that the AGE/Ca^{2+} complexes facilitate the crossing of cell and mitochondrial membranes resulting in an increase in the level of intracellular and mitochondrial calcium.

Since alteration of the mitochondrial membrane potential would possibly trigger apoptotic signal transduction, we then determined whether AGEs could cause mitochondrial depolarization by using the JC-1 probe. We found more than 41 % of the cells preincubated with **BAA-1** exhibited lower mitochondrial membrane potential. In contrast, 7.0 and 24.1 % of the cells preincubated with **MAA-1** or **NAA-1** had lower mitochondrial membrane potential (Figure S10 in the Supporting Information). The results suggested that the higher cytotoxicity of **BAA-1** very likely arises from the strongest ability to upregulate the level of mitochondrial calcium and to cause mitochondrial depolarization (but might also, in part, be because of complex I inhibition).

We compared the changes in the intracellular calcium level of HepG2 cells preincubated with AGEs with the thermodynamic statistics obtained from AGE/Ca^{2+} ITC data. The results of ITC indicated that the chelating enthalpy of **BAA-1** was stronger than that of **MAA-1** and **NAA-1**, and **BAA-1** increased the intracellular levels of calcium to the highest extent (BAAs > NAAs > MAAs; Figure 3). Indeed, the results are consistent with our previous observation that **BAA-1** can induce a transient but strong increase in the Ca^{2+}-activated K^+ current in cultured smooth-muscle cells without altering single-channel conductance.[15] Although, in the current study, the ion transport of AGEs was not detectable using a W-08 apparatus,[16] we showed here using an EDTA competitive assay that the presence of Ca^{2+} ions affected the bioactivity of AGEs. In addition, analysis of our ITC data indicated that the chelating enthalpy of **BAA-1**/Ca^{2+} (5.7 kcal mol^{-1}) was stronger than that of **MAA-1** and **NAA-1** (2.3 and 1.5 kcal mol^{-1}, respectively, Figure 1 d–f). These thermal statistics indicate that the calcium-chelation ability of **BAA-1** is the strongest among all the AGEs tested.

Based on the binding molar ratio of BAAs/Ca^{2+} of 2 and the lowest conformer of **BAA-1** from ab initio calculations,[17] we propose a model in which two **BAA-1** molecules in an L-shaped conformation (shown as a crisscrossed structure in Figure 5) can chelate with a Ca^{2+} ion using the adjacent hydroxy/THF moieties and hide the hydrophilic surface of the AGE molecules. In other words, the membrane-penetration ability of **BAA-1** can be enhanced through dissimulation of the polar functional groups of hydroxy/THF moieties, while complexes are formed that express the peripheral hydrophobic surface of AGEs. In this way, the **BAA-1**/Ca^{2+} complex can diffuse across cellular and mitochondrial membranes to disrupt the intracellular calcium levels and to mediate higher cytotoxicity. In contrast, in the **MAA-1**/Ca^{2+} and **NAA**-1/Ca^{2+} complexes, with binding molar ratios of 1 and 3, respectively, the polar groups may still be partially exposed and would thereby reduce the hydrophobic surfaces. Therefore, MAAs and NAAs with lower calcium-chelation ability and more hydrophilic surfaces on the complex surfaces

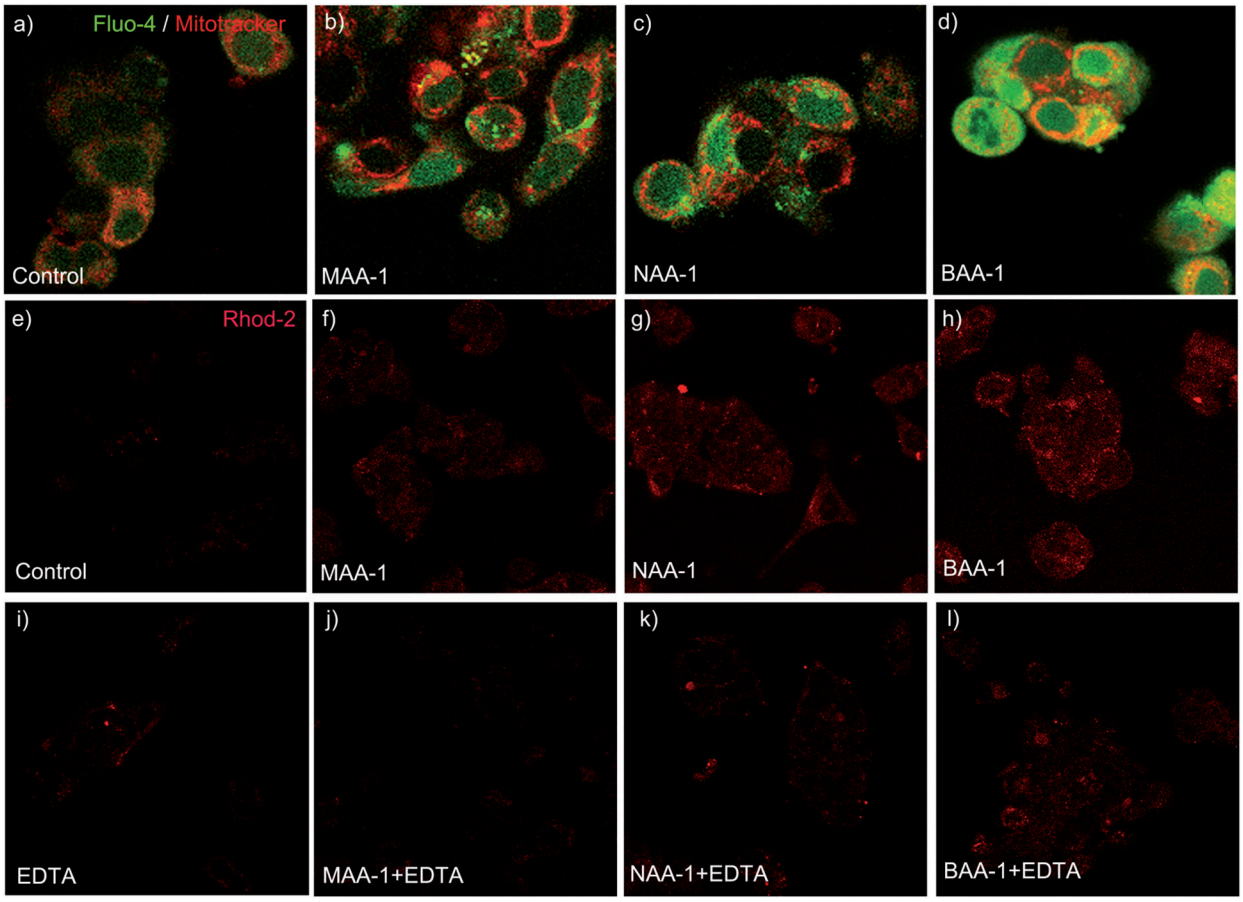

Figure 4. AGEs increase the intracellular level of calcium. a–d) HepG2 cells were prestained with 0.5 μM MitoTracker Red 580 FM for 45 min and then incubated with 50 μM **NAA-1**, **BAA-1**, or **MAA-1** for another 10 min. Subsequently, 2 μM Fluo-4 AM solution was added. e–h) HepG2 cells were incubated with 50 μM **NAA-1**, **BAA-1**, or **MAA-1** for 10 min, and then stained with 2 μM Rhod-2/AM at 25 °C for 20 min. i–l) HepG2 cells were preincubated with 5 mM EDTA for 30 min, followed by incubation with 50 μM **NAA-1**, **BAA-1**, or **MAA-1** for 10 min. The cells were then stained with 2 μM Rhod-2/AM at 25 °C for 20 min. The fluorescence images were obtained after 20 min using a confocal microscope.

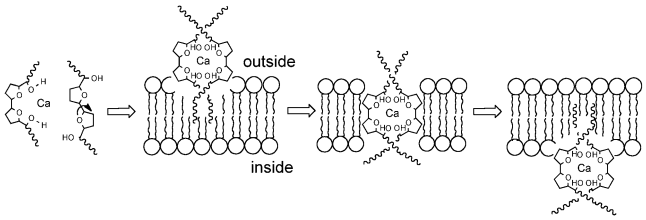

Figure 5. Calcium-chelation model for an adjacent bis-THF **BAA-1**/Ca^{2+} complex that enhances cell-membrane penetration. The lipid bilayer can be that of the cell membrane or the mitochondrial membrane.

would display lower cytotoxicity. This is exemplified by **MAA-3**, which did not chelate Ca^{2+} and was less toxic. Judging from the previous report[3] and our results presented herein, disruption of intracellular calcium homeostasis and inhibition of the electron system in mitochondrial complex I may synergistically mediate cell cytotoxicity.

Intracellular calcium overload is known to contribute to neurodegenerative tauopathy, which causes several human pathological conditions and possibly neurodegenerative disorders such as Alzheimer's,[18] Huntington's, and motor neurone diseases.[19] Moreover, some AGEs have been affiliated with sporadic neurodegenerative tau pathologies.[20] Our studies attempted to support the findings that **MAA-1**, one of the abundant mono-AGEs,[21] shows neurotoxicity in several in vitro and in vivo paradigms.[22] Interestingly, three special mono-THF AGEs with free OH-15 and OAc-17 showed an EC_5-Tau effect similar to that of **BAA-1** and **BAA-2**. In view of our proposed model, the space between OH-15 (instead of OH-17) and OH-22 would be similar to that between OH-15 and OH-24 in **BAA-1** and **BAA-2** (roll-iniastatin 2) for chelating Ca^{2+} ions.

In summary, Ca^{2+} ions play an important role in the regulation of many cellular functions and the activation of many enzymes. Therefore, the intracellular and extracellular concentrations of Ca^{2+} ions are strictly regulated, although the concentration of calcium in the cytosol is as low as about 10^{-7} M. Our current work reveals that the mechanism underlying the cytotoxicity of AGEs is modulated by the chelation of THF moieties of AGEs with Ca^{2+} to form hydrophobic complexes. The calcium chelation of AGEs correlates with their levels of cytotoxicity. We further revealed that incubation of cells with bis-THF AGEs can also increase mitochondrial Ca^{2+} concentrations and decrease the mitochondrial membrane potential, which is very likely the main cause of

higher cytotoxicity. Therefore, the ability of AGE/Ca^{2+} complexes to modulate intracellular and mitochondrial calcium levels may offer an opportunity to develop a new strategy targeting Ca^{2+}-dependent signaling pathways.

Experimental Section

Materials: AGEs were isolated from Formosan Annonaceous plants including *Annona muricata*, *A. montana*, *A. squamosa*, *A. reticulata*, and *Rollinia mucosa*. Annonacin (**MAA-1**) and (+)-monhexocin (**LAA**) were isolated from *A. montana*.[23] Muricin H (**MAA-3**) was isolated from *A. muricata*.[24] Squamostatin A (**NAA-1**) and squamocin (**BAA-1**) were isolated from *A. atemoya*.[25] Uvariamicin-I (**MAA-2**), bullatanocin (**NAA-2**), and bullatacin (**BAA-2**) were isolated from *A. squamosa*. **MAA-3** and **LAA** are new compounds. **MAA-2** was isolated and purified from the analogues uvariamicin-II and -III.[26] All of the AGEs were repurified by reversed-phase HPLC before bioevaluation (> 99 %).

Complex formation of AGE/calcium ion analyzed by ITC: The measurements were conducted on a VP-ITC microcalorimeter (Microcal, Inc., Northampton, Mass., USA). In the assays, 1) 0.03 mM calcium perchlorate (1.436 mL in $CH_3CN/CHCl_3$) was mixed with 1 mM **MAA-1** (300 μL in the same mixing solvent); 2) 0.03 mM calcium perchlorate (1.436 mL in CH_3CN) was mixed with 1 mM **NAA-1** (300 μL in CH_3CN); and 3) 0.065 mM calcium perchlorate (1.436 mL in CH_3CN) was mixed with 1 mM **BAA-1** (300 μL in CH_3CN), all at 25 °C with continuous stirring (300 rpm). The heat produced during complex formation was analyzed using Origin software (Edition 7.0, Microcal Inc.). The integration of the heat pulses obtained from each titration were fitted to a one-site binding curve to obtain a nonlinear least-squares algorithm (minimization of χ^2), the enthalpy change (ΔH in cal mol^{-1}), the entropy change (ΔS in cal mol^{-1} K^{-1}), the association constant (K_{ass} in M^{-2}), and the number of binding sites (N, per compound).

Apoptosis and cytotoxicity assays: HepG2 cells (30×10^3 cells per well) were seeded in a 96-well plate. The samples were preincubated either with or without 10 nM EDTA. Then **NAA-1**, **BAA-1**, or **MAA-1** dissolved in dimethyl sulfoxide (DMSO) at different concentrations was added. After incubation of untreated or AGE-treated cells for 48 h, the cells were washed once with phosphate-buffered saline (PBS), and were then incubated with 3-(4,5-dimethylthiazol-2-yl)-2,5-diphenyltertrazolium bromide (MTT, Sigma, 1 mg mL^{-1}, 50 μL per well) at 37 °C for 2 h. DMSO (150 μL per well) was added at room temperature to dissolve the blue-violet formazan deposit. The absorbance at 570 nm was measured with an ELISA reader. To measure the apoptotic cells, cells were pretreated with **NAA-1**, **BAA-1**, or **MAA-1** for 6 h. The cells were then collected, washed with PBS, and co-stained with fluorescein isothiocyanate (FITC)-conjugated annexin V antibodies (BD Biosciences) and propidium iodide (Sigma) for 15 min. The fluorescence of FITC and propidium iodide was analyzed using a FACSCalibur instrument (BD Biosciences).

Determination of mitochondrial calcium uptake:[27] HepG2 cells were pretreated with **NAA-1**, **BAA-1**, or **MAA-1** for 10 min, followed by staining with 2 μM Rhod-2/AM at 25 °C for 20 min. Cells were then washed with Hank's Balanced Salt Solution (HBSS) containing 2 % fetal bovine serum (FBS) and 10 mM 4-(2-hydroxyethyl)-1-piperazineethanesulfonic acid (HEPES), and fluorescence images were obtained using a temperature-controlled stage and confocal microscope.

Determination of the intracellular level of calcium:[28] Intracellular free calcium concentrations were measured using the fluorescent indicator dye Fluo-4 AM, the membrane-permeable acetoxymethyl ester form of Fluo-4. Fluo-4 NW calcium assay kits and Fluo-4 AM were purchased from Molecular Probes, Inc. HepG2 cells grown in a 96-well plate were pretreated with **NAA-1**, **BAA-1**, or **MAA-1** for 10 min at room temperature. The medium was removed and Fluo-4 AM solution (100 μL) was added to each well; the plates were incubated at 37 °C for 30 min, and then at room temperature for 10 min. The excitation of Fluo-4 AM fluorescence was set at 494 nm, and the fluorescence emission at 560 nm was measured. The changes in calcium levels are given as fold changes in the optical density value. To monitor the changes in the level of cytosolic and mitochondrial Ca^{2+}, HepG2 cells were seeded at 1×10^5 cells per 35 mm glass Petri dish and allowed to attach for 24 h. The cells were then prestained with 0.5 μM MitoTracker Red 580 FM for 45 min. The medium was replaced with medium containing **NAA-1**, **BAA-1**, or **MAA-1**, and the samples were incubated for 10 min, followed by addition of 2 μM Fluo-4 AM solution. Fluorescence images were obtained every 1 min for a 30 min period using time-lapse confocal microscopy (Leica confocal microscope SP2, Leica Microsystems, Milton Keynes, UK).

Received: January 28, 2011
Published online: July 8, 2011

Keywords: acetogenins · calcium · chelates · cytotoxicity · isothermal titration calorimetry

[1] H. Makabe, H. Konno, H. Miyoshi, *Curr. Drug Discovery Technol.* **2008**, *5*, 213 – 229.
[2] Y. Nakanishi, F.-R. Chang, C.-C. Liaw, Y.-C. Wu, K. F. Bastow, K.-H. Lee, *J. Med. Chem.* **2003**, *46*, 3185 – 3188.
[3] A. Bermejo, B. Figadère, M.-C. Zafra-Polo, I. Barrachina, E. Estornell, D. Cortes, *Nat. Prod. Rep.* **2005**, *22*, 269 – 303.
[4] a) S. Derbré, G. Roué, E. Poupon, S. A. Susin, R. Hocquemiller, *ChemBioChem* **2005**, *6*, 979 – 982; b) H.-X. Liu, G.-R. Huang, H.-M. Zhang, S. Jiang, J.-R. Wu, Z.-J. Yao, *ChemBioChem* **2007**, *8*, 172 – 177; c) K. Sekiguchi, M. Murai, H. Miyoshi, *Biochim. Biophys. Acta Bioenerg.* **2009**, *1787*, 1106 – 1111.
[5] H. Miyoshi, M. Ohshima, H. Shimada, T. Akagi, H. Iwamura, J. L. McLaughlin, *Biochim. Biophys. Acta Bioenerg.* **1998**, *1365*, 443 – 452.
[6] a) M. Murai, N. Ichimaru, M. Abe, T. Nishioka, H. Miyoshi, *Biochemistry* **2006**, *45*, 9778 – 9787; b) M. J. Rieser, J. F. Kozlowski, K. V. Wood, J. L. McLaughlin, *Tetrahedron Lett.* **1991**, *32*, 1137 – 1140; c) Z.-J. Yao, H.-P. Wu, Y.-L. Wu, *J. Med. Chem.* **2000**, *43*, 2484 – 2487.
[7] N. Kojima, T. Morioka, D. Urabe, M. Yano, Y. Suga, N. Maezaki, A. Ohashi-Kobayashi, Y. Fujimoto, M. Maeda, T. Yamori, T. Yoshimitsu, T. Tanaka, *Bioorg. Med. Chem.* **2010**, *18*, 8630 – 8641.
[8] a) S. Derbré, R. Duval, G. Roué, A. Garofano, E. Poupon, U. Brandt, S. A. Susin, R. Hocquemiller, *ChemMedChem* **2006**, *1*, 118 – 129; b) N. Kojima, T. Tanaka, *Molecules* **2009**, *14*, 3621 – 3661.
[9] S. Derbré, S. Gil, M. Taverna, C. Boursier, V. Nicolas, E. Demey-Thomas, J. Vinh, S. A. Susin, R. Hocquemiller, E. Poupon, *Bioorg. Med. Chem. Lett.* **2008**, *18*, 5741 – 5744.
[10] a) C. M. Deber, D. R. Pfeiffer, *Biochemistry* **1976**, *15*, 132 – 141; b) B. J. Abbott, D. S. Fukuda, D. E. Dorman, J. L. Occolowitz, M. Debono, L. Farhner, *Antimicrob. Agents Chemother.* **1979**, *16*, 808 – 812; c) C. J. Dutton, B. J. Banks, C. B. Cooper, *Nat. Prod. Rep.* **1995**, *12*, 165 – 181.
[11] a) S. Sasaki, H. Naito, K. Maruta, E. Kawahara, M. Maeda, *Tetrahedron Lett.* **1994**, *35*, 3337 – 3340; b) S. Sasaki, K. Maruta, H. Naito, H. Sugihara, K. Hiratani, M. Maeda, *Tetrahedron Lett.* **1995**, *36*, 5571 – 5574; c) S. Sasaki, K. Maruta, H. Naito, R. Maemura, E. Kawahara, M. Maeda, *Tetrahedron* **1998**, *54*, 2401 – 2410; d) J.-F. Peyrat, B. Figadère, A. Cavé, J. Mahuteau, *Tetrahedron Lett.* **1995**, *36*, 7653 – 7656.
[12] J.-F. Peyrat, J. Mahuteau, B. Figadère, A. Cavé, *J. Org. Chem.* **1997**, *62*, 4811 – 4815.

[13] J. E. Ladbury, B. Z. Chowdhry, *Chem. Biol.* **1996**, *3*, 791 – 801.
[14] C.-C. Liaw, Y.-L. Yang, M. Chen, F.-R. Chang, S.-L. Chen, S.-H. Wu, Y.-C. Wu, *J. Nat. Prod.* **2008**, *71*, 764 – 771.
[15] S.-N. Wu, H.-T. Chiang, F.-R. Chang, C.-C. Liaw, Y.-C. Wu, *Chem. Res. Toxicol.* **2003**, *16*, 15 – 22.
[16] H. Araya, Y. Fujimoto, K. Hirayama, *Yuki Gosei Kagaku Kyokaishi* **1994**, *52*, 765 – 777.
[17] J. A. Bombasaro, M. F. Masman, L. N. Santagata, M. L. Freile, A. M. Rodríguez, R. D. Enriz, *J. Phys. Chem. A* **2008**, *112*, 7426 – 7438.
[18] a) M. Kawahara, M. Negishi-Kato, Y. Sadakane, *Expert Rev. Neurother.* **2009**, *9*, 681 – 693; b) D. H. Small, R. Gasperini, A. J. Vincent, A. C. Hung, L. Foa, *J. Alzheimer's Dis.* **2009**, *16*, 225 – 233.
[19] a) D. W. Choi, *J. Neurobiol.* **1992**, *23*, 1261 – 1276; b) D. W. Choi, *Ann. N. Y. Acad. Sci.* **1994**, *747*, 162 – 171.
[20] M. Höllerhage, A. Matusch, P. Champy, A. Lombes, M. Ruberg, W. H. Oertel, G. U. Höglinger, *Exp. Neurol.* **2009**, *220*, 133 – 142.
[21] a) D. Caparros-Lefebvre, A. Elbaz, *Lancet* **1999**, *354*, 281 – 286; b) E. Apartis, B. Gaymard, S. Verhaeghe, E. Roze, M. Vidailhet, A. Lannuzel, *Brain* **2008**, *131*, 2701 – 2709.
[22] a) A. Lannuzel, P. P. Michel, G. U. Höglinger, P. Champy, A. Jousset, F. Medja, A. Lombès, F. Darios, C. Gleye, A. Laurens, R. Hocquemiller, E. C. Hirsch, M. Ruberg, *Neuroscience* **2003**, *121*, 287 – 296; b) P. Champy, G. U. Höglinger, J. Feger, C. Gleye, R. Hocquemiller, A. Laurens, V. Guerineau, O. Laprévote, F. Medja, A. Lombes, P. Michel Patrick, A. Lannuzel, C. Hirsch Etienne, M. Ruberg, *J. Neurochem.* **2004**, *88*, 63 – 69; c) M. Escobar-Khondiker, M. Höllerhage, M. P. Muriel, P. Champy, A. Bach, C. Depienne, G. Respondek, E. S. Yamada, A. Lannuzel, T. Yagi, E. C. Hirsch, W. H. Oertel, R. Jacob, P. P. Michel, M. Ruberg, G. U. Höglinger, *J. Neurosci.* **2007**, *27*, 7827 – 7837.
[23] C.-C. Liaw, F.-R. Chang, S.-L. Chen, C.-C. Wu, K.-H. Lee, Y.-C. Wu, *Bioorg. Med. Chem.* **2005**, *13*, 4767 – 4776.
[24] C.-C. Liaw, F.-R. Chang, C.-Y. Lin, C.-J. Chou, H.-F. Chiu, M.-J. Wu, Y.-C. Wu, *J. Nat. Prod.* **2002**, *65*, 470 – 475.
[25] F.-R. Chang, J.-L. Chen, C.-Y. Lin, H.-F. Chiu, M.-J. Wu, Y.-C. Wu, *Phytochemistry* **1999**, *51*, 883 – 889.
[26] A. Hisham, L. A. C. Pieters, M. Claeys, E. Esmans, R. Dommisse, A. J. Vlietinck, *Tetrahedron Lett.* **1990**, *31*, 4649 – 4652.
[27] a) B. J. Hawkins, L. A. Solt, I. Chowdhury, A. S. Kazi, M. R. Abid, W. C. Aird, M. J. May, J. K. Foskett, M. Madesh, *Mol. Cell. Biol.* **2007**, *27*, 7582 – 7593; b) A. M. Hofer, T. E. Machen, *Am. J. Physiol.* **1994**, *267*, G442 – G451.
[28] A. W. Simpson, *Methods Mol. Biol.* **2006**, *312*, 3 – 36.

